

Two Germanide Hydride Phases Grown in Calcium-Rich Flux: Use of Interstitial Elements for Discovery of New Phases

David A. Lang^[a] and Susan E. Latturmer^{*[a]}

Dedicated to Professor John D. Corbett on the occasion of his 85th birthday

Keywords: Zintl phases / Hydrides / Interstitials / Crystal growth / Flux growth

Reactions of germanium in calcium/lithium flux yield crystals of new complex hydrides, with hydrogen incorporated either inadvertently due to traces of hydride contaminants in the flux metals, or deliberately by the addition of CaH_2 as a reactant. The new germanide hydride Zintl phase $\text{LiCa}_7\text{Ge}_3\text{H}_3$ crystallizes in the orthorhombic space group $Pnma$ [$a = 9.8599(2)$ Å, $b = 13.7716(3)$ Å, $c = 8.7430(2)$ Å; $Z = 4$; $R_1 = 0.0195$]. The structure features isolated Ge^{4-} anions surrounded by calcium ions, and hydride anions in octahedral

sites defined by Ca and Li ions. Another product that appears in these reactions was found to form from incorporation of both oxide and hydride impurities. This phase, $\text{LiCa}_{11}\text{Ge}_3\text{OH}_x$ ($x \approx 4$) forms in the tetragonal space group $P4_2/nmc$ [$a = 15.832(2)$ Å, $c = 13.694(2)$ Å; $Z = 8$; $R_1 = 0.0350$]. In addition to isolated Ge^{4-} and octahedral H^- anions, the structure also features incorporation of oxide anions in octahedral sites.

Introduction

Extensive work by the Corbett research group on alkaline-earth-rich Zintl phases and intermetallics has indicated the ubiquitous nature of impurities and interstitial atoms and their importance in stabilizing many new phases.^[1–7] Incorporation of hydride anions is of particular interest; the difficulty in detecting this element in X-ray crystallography studies has led to reports of phases with ostensibly electron-rich structures and stoichiometries. Compounds such as $\text{Ba}_{21}\text{M}_2\text{O}_5$ ($\text{M} = \text{Ge}, \text{Si}$) and Ba_5Ga_6 were found to have incorporated hydrides, leading to their reclassification as charge-balanced Zintl phases ($\text{Ba}_{21}\text{M}_2\text{O}_5\text{H}_{24}$ and $\text{Ba}_5\text{Ga}_6\text{H}_2$, respectively).^[3,4] Careful and systematic studies of the $\text{AE}_5\text{Pn}_3\text{H}_x$ and $\text{AE}_5\text{Tt}_3\text{H}_x$ systems ($\text{AE} = \text{Ca}, \text{Sr}, \text{Ba}, \text{Yb}, \text{Eu}$; $\text{Pn} = \text{pnictide}$; $\text{Tt} = \text{tetrelide}$) by using X-ray and neutron diffraction evidenced the importance of the presence of hydride; in its absence, different structures are formed.^[5–7]

Hydride incorporation is particularly endemic to compounds rich in calcium, strontium, and barium. In their elemental form, these alkaline earth metals react with traces of water to form metal hydroxides and hydrogen; the hydrogen reacts with the metal to form hydrides. As a result of this,

commercial samples of these metals, even if carefully packaged, may contain significant amounts of hydride and oxide contaminants.^[8] The use of these contaminated metals as reactants may lead to incorporation of hydride and oxide interstitials into products. This is particularly problematic if the metals are used in large amounts, for instance, as a reaction medium in metal flux syntheses.^[9] We have been exploring the use of calcium-rich mixtures for this purpose. Equimolar mixtures of calcium and lithium melt at 300 °C and dissolve a wide range of metallic and metalloid reactants. Reactions of carbon in Ca/Li flux made from commercially available (and hydride-contaminated) calcium metal led to our recent discovery of the new carbide hydride $\text{LiCa}_2\text{C}_3\text{H}$, which features C_3^{4-} and H^- anions. Subsequent reactions with added CaH_2 increased the yield of this phase.^[10]

The continuation of this work, using germanium instead of carbon, has led to the formation of two new phases reported herein. Germanium reacts with CaH_2 in Ca/Li flux to form $\text{LiCa}_7\text{Ge}_3\text{H}_3$; a Zintl phase hydride. In the presence of oxide contamination (or deliberate addition of CaO as a reactant), the formation of $\text{LiCa}_{11}\text{Ge}_3\text{OH}_x$ ($x \approx 4$) is observed. Both structures feature isolated Ge^{4-} anions coordinated to 9–10 calcium cations, and hydride anions octahedrally coordinated by Ca^{2+} and Li^+ ions. The $\text{LiCa}_{11}\text{Ge}_3\text{OH}_4$ phase does not appear to be charge-balanced and has a complex structure that, in addition to Ge^{4-} and H^- anions, also features oxide anions octahedrally coordinated by calcium cations.

[a] Department of Chemistry and Biochemistry, Florida State University, Tallahassee, FL 32308, USA
Fax: +1-850-644-8281
E-mail: latturmer@chem.fsu.edu

Results and Discussion

Synthesis

Synthetic explorations in Ca/Li flux indicate that this reaction medium is an excellent solvent for a wide range of metals and metalloids. It also dissolves ionic compounds such as Ca_3N_2 and CaH_2 . To explore the effects of oxide and hydride impurities, reactions of germanium were carried out in Ca/Li flux under a variety of conditions: using commercial Ca to form the flux, using distilled Ca to form the flux, and with or without deliberate addition of CaH_2 or CaO as reactants.

Because of the high reactivity and volatility of both flux components, crucible selection is limited to sealed metal ampoules. Steel ampoules are stable to the flux and were used in this work. One drawback of steel is the possibility of leaching iron, carbon, and other alloying elements from the ampoule walls; this is particularly problematic if magnetic measurements are planned on the products. While no iron was indicated by SEM-EDS (energy-dispersive spectroscopy) measurements, incorporation of even trace amounts of iron would affect magnetic data. Niobium or tantalum ampoules are recommended to avoid such contamination; however, at elevated temperatures, these ampoules become permeable to hydrogen. This property has been used to remove hydride impurities from metals.^[2]

Since synthesis in Ca/Li flux favors the formation of calcium-rich phases that incorporate a range of interstitial elements, it is extremely difficult to control the synthesis to isolate only one of the observed calcium- and germanium-containing products (Ca_2Ge , $\text{LiCa}_7\text{Ge}_3\text{H}_3$, and $\text{LiCa}_{11}\text{Ge}_3\text{OH}_4$). Pure Ca_2Ge can be obtained in a well-crystallized form from reaction of Ge in Ca/Li flux made with distilled Ca; the unit-cell parameters of these crystals match those reported in the literature for the orthorhombic structure.^[11] Similar reactions in commercial Ca/Li flux lead predominantly to Ca_2Ge , but small amounts of $\text{LiCa}_7\text{Ge}_3\text{H}_3$ and $\text{LiCa}_{11}\text{Ge}_3\text{OH}_4$ are also present. The yield of $\text{LiCa}_7\text{Ge}_3\text{H}_3$ is greatly increased by using distilled Ca/Li and Ge and CaH_2 as reactants; this supplies a large excess of hydride (lowering the amount of binary Ca_2Ge formed) and eliminates oxide contaminants, which can lead to the formation of $\text{LiCa}_{11}\text{Ge}_3\text{OH}_4$. Similar reactions of Ge and CaH_2 , carried out in commercial Ca/Li flux, also lead to increased amounts of the $\text{LiCa}_7\text{Ge}_3\text{H}_3$ phase, but the $\text{LiCa}_{11}\text{Ge}_3\text{OH}_4$ phase is produced as well as a result of the oxide present in commercial calcium. Recrystallized CaH_2 is also observed as a product, as seen in the previously reported synthesis of $\text{LiCa}_2\text{C}_3\text{H}$.^[10] Reactions of CaH_2 , CaO, and Ge in the Ca/Li flux yield a mixture of several phases, with $\text{LiCa}_{11}\text{Ge}_3\text{OH}_4$ being predominant, but $\text{LiCa}_7\text{Ge}_3\text{H}_3$, CaH_2 , and Ca_2Ge are also present. These results underscore the importance of using distilled calcium, but also indicate the usefulness of exploring the deliberate addition of interstitial elements for materials discovery.

Structural Description

$\text{LiCa}_7\text{Ge}_3\text{H}_3$ is a charge-balanced Zintl phase comprised of isolated Ge^{4-} and H^- anions and Ca^{2+} and Li^+ cations. This phase crystallizes in an orthorhombic structure, shown in Figure 1, which can be viewed as layers of Ca/Ge separated by slabs containing both germanium and hydride anions, as well as Li^+ cations. In the Ca/Ge slab, Ge(1) atoms are coordinated by 10 calcium atoms at distances ranging from 3.04 to 3.68 Å (see Table 1); the Ge–Ca interatomic distances in Ca_2Ge and Ca_5Ge_3 are also in this range.^[2,11] The Ge(2) atoms in the hydride slab are coordinated more strongly to 6 calcium atoms in a trigonal-prismatic distribution with bond lengths of 2.93–2.96 Å. These trigonal prisms share edges with hydride-centered octahedra to form the hydride germanide slabs (see Figure 2).

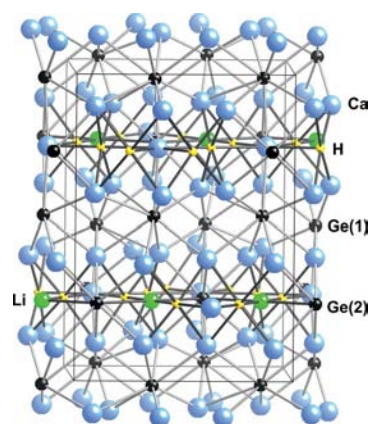


Figure 1. Orthorhombic structure of $\text{LiCa}_7\text{Ge}_3\text{H}_3$ viewed along the c axis.

Table 1. Comparison of selected interatomic distances in $\text{LiCa}_7\text{Ge}_3\text{H}_3$ and $\text{LiCa}_{11}\text{Ge}_3\text{OH}_4$.

Bonds in $\text{LiCa}_7\text{Ge}_3\text{H}_3$	Length [Å]	Bonds in $\text{LiCa}_{11}\text{Ge}_3\text{OH}_4$	Length [Å]
Ge(1)–Ca	3.0439(3)–3.6861(3)	Ge(1)–Ca	2.945(2)–3.286(1)
Ge(2)–Ca	2.9321(3)–2.9639(3)	Ge(2)–Ca	3.154(2)–3.376(2)
Ge(2)–Li(1)	2.800(4), 2.997(4)	Ge(3)–Ca	3.039(1)–3.500(1)
H(1)–Li(1)	2.11(3)	H(1)–Li(10)	2.255(5)
H(1)–Ca	2.49(2)–2.63(2)	H(1)–Ca(9)	2.280(2)
H(2)–Ca	2.44(2)–2.62(2)	H(2)–Ca	2.30(3)–2.64(4)
H(3)–Li(1)	2.14(3)	H(3)–Ca	2.45(4)–2.75(5)
H(3)–Ca	2.44(3)–2.67(2)	O(1)–Ca	2.371(1)–2.408(1)

All three hydride sites in the structure are octahedrally coordinated by cations. Although tetrahedral coordination is more common for hydride anions due to their small size,^[6,12] octahedral coordination is seen in $\text{LiCa}_2\text{C}_3\text{H}$, $\text{Ba}_9\text{In}_4\text{H}$, $\text{Ca}_6[\text{Cr}_2\text{N}_6]\text{H}$, and $\text{AE}_3\text{Pn}_5\text{H}_x$ hydrides with the stuffed Mn_5Si_3 -type such as $\text{Sr}_5\text{As}_3\text{H}$.^[10,13,14] $\text{Ca}_6[\text{Cr}_2\text{N}_6]\text{H}$ and $\text{LiCa}_2\text{C}_3\text{H}$ exhibit Ca–H distances of 2.6491(4) and 2.5016(1) Å, respectively. These are within the range of Ca–H distances seen in $\text{LiCa}_7\text{Ge}_3\text{H}_3$. The octahedral site of the hydrides in $\text{LiCa}_7\text{Ge}_3\text{H}_3$ (and $\text{LiCa}_2\text{C}_3\text{H}$) may be stabilized by the presence of Li^+ in the coordination sphere. Of the

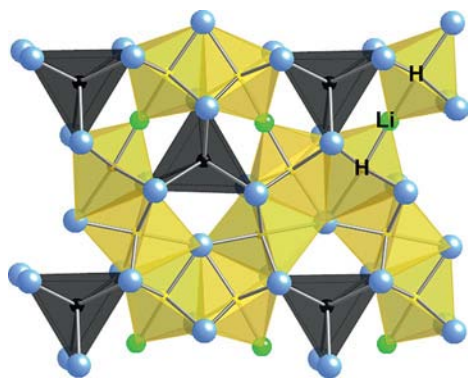


Figure 2. Polyhedral representation of the hydride layer in $\text{LiCa}_7\text{Ge}_3\text{H}_3$, viewed along the b axis. Hydride-centered octahedra are in yellow; germanium-centered trigonal prisms in black.

three hydride sites in the structure, two of them [H(1) and H(2)] are coordinated to five Ca^{2+} cations and one Li^+ ion. The lithium site is shared between these octahedra, resulting in a linear H–Li–H unit with Li–H distances of 2.11(3) and 2.14(3) Å. While these Li–H distances are longer than the 1.875 Å bond length observed in $\text{LiCa}_2\text{C}_3\text{H}$, it is notable that the carbide hydride structure also features a structural motif of lithium hydride chains (in that case, an infinite H–Li–H–Li– chain running along the c axis), as does the $\text{LiCa}_{11}\text{Ge}_3\text{OH}_4$ structure (see below). Band-structure calculations and electron-localization-function studies on $\text{LiCa}_2\text{C}_3\text{H}$ indicated an interaction between Li and H, which may have promoted formation of chains and clusters of Li and H in these structures.^[10]

The presence of oxide in the Ca/Li/Ge/ CaH_2 reaction mixture leads to the formation of $\text{LiCa}_{11}\text{Ge}_3\text{OH}_4$. This phase has a tetragonal structure featuring isolated Ge^{4-} , O^{2-} , and H^- anions coordinated by Ca^{2+} and Li^+ . The presence of several different anions results in a highly complex structure; this is also demonstrated by $\text{Ba}_{21}\text{Ge}_2\text{O}_5\text{H}_{24}$ (which features the same set of anions) and $\text{Sr}_{21}\text{Si}_2\text{O}_5\text{C}_6$ (which is related to the barium phase by replacing the hydride anions with carbide anions).^[3,15] The $\text{LiCa}_{11}\text{Ge}_3\text{OH}_4$ structure is shown in Figures 3 and 4. In Figure 3 the Ge-centered polyhedra are featured; in Figure 4, the hydride-

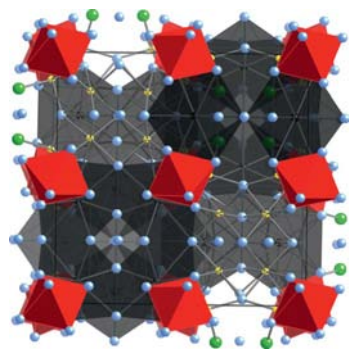


Figure 3. The $\text{LiCa}_{11}\text{Ge}_3\text{OH}_4$ structure, viewed along the c axis. Ge^{4-} coordination spheres represented as gray polyhedra and oxide-centered octahedra in red. Calcium, lithium, and hydrogen atoms are blue, green, and yellow, respectively.

centered octahedra are highlighted. The three Ge^{4-} anion sites are coordinated by 9–10 Ca^{2+} atoms with Ge–Ca interatomic distances similar to those in $\text{LiCa}_7\text{Ge}_3\text{H}_3$ (see Table 1). The oxide anions are octahedrally coordinated by calcium ions, with a small range of Ca–O distances only slightly longer than the 2.37 Å observed in the inverse perovskite Ca_3GeO .^[16]

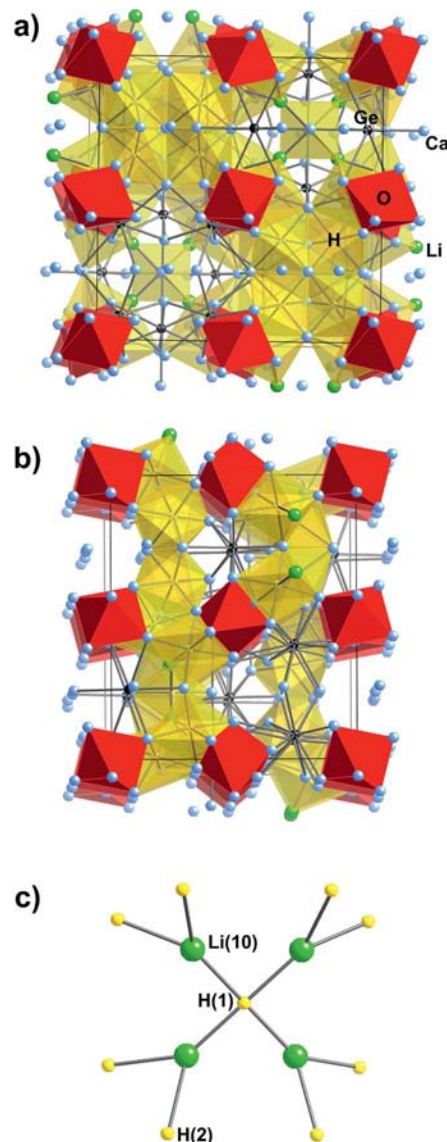


Figure 4. $\text{LiCa}_{11}\text{Ge}_3\text{OH}_4$ structure, highlighting the locations and connectivity of the hydride-centered octahedra (yellow). (a) Structure viewed along the c axis. (b) Structure viewed along the a axis. (c) Lithium hydride cluster.

The stoichiometry of $\text{LiCa}_{11}\text{Ge}_3\text{OH}_4$ is not charge-balanced; it is possible that more hydride is incorporated in the compound but is not found in the structural refinement. While three single-crystal X-ray diffraction datasets of this phase were analyzed and compared to locate consistent hydride sites (see the Experimental Section), it is likely that some have been missed, particularly if the hydride ions are distributed over several partially occupied sites. Of the samples analyzed by powder and single-crystal diffraction, the

unit cells did not vary significantly with the reactant ratio, which may indicate that this compound is a Zintl phase with no significant phase width. Neutron diffraction studies on deuterium analogues would be of great benefit to determine the true hydride (deuteride) content. Synthesis of a fluoride analogue ($\text{LiCa}_{11}\text{Ge}_3\text{OF}_x$) would also aid in the structural analysis; F^- can in many cases occupy hydride sites, and this heavier atom is easier to locate in crystal structure refinement.^[2,7] However, reactions of Ge, CaO, and CaF_2 have not yielded isostructural products.

Three hydride sites were definitively located in the structure. All three are octahedrally coordinated, with a wider range of Ca–H and Li–H distances than those seen for charge-balanced $\text{LiCa}_7\text{Ge}_3\text{H}_3$. In particular, two shorter Ca–H bonds are observed [2.280(2) and 2.30(3) Å]. However, these bond lengths compare well to the 2.30–2.36 Å range seen in CaH_2 , and to the sum of the ionic radii for these elements.^[10,17] The hydride-centered octahedra share edges and faces to form hydride layers in the *ab* plane (see Figure 4b). It is notable that the mixed Li(10)/Ca(10) site is adjacent to two of these hydride sites, resulting in the formation of an H–Li–H–Li–H cluster in the structure (Figure 3c). The Li–H bonds are longer than expected, which is likely to be due to the mixing of Ca on the Li site.

Conclusions

Synthesis in alkaline-earth-rich metal fluxes has proven to be a useful technique for the discovery of new Zintl phases and polar intermetallics. Hydride contamination in calcium and other alkaline earths is often viewed as problematic, but deliberate addition of CaH_2 in reactions can lead to the discovery of new complex hydrides. Reactions of germanium with CaH_2 and CaO in Ca/Li flux produce $\text{LiCa}_7\text{Ge}_3\text{H}_3$ and $\text{LiCa}_{11}\text{Ge}_3\text{OH}_x$; both structures feature isolated Ge^{4-} and H^- anions. Another structural feature these phases share is the clustering of lithium and hydride sites. Lithium lowers the melting point of the flux, and it may also promote the formation of Li–H-rich regions in the structures growing from the melt. Additional hydride sites are likely to be present in $\text{LiCa}_{11}\text{Ge}_3\text{OH}_x$ to balance the charge of the metal cations; the synthesis of deuterium or fluoride analogues is being attempted to clarify this issue.

Experimental Section

Syntheses: All manipulations of air-sensitive reactants and products were carried out in an argon-filled glovebox. Reactants included calcium shot (99.5%, Alfa Aesar), lithium rod (99.8%, Strem Chemicals), calcium hydride powder (98%, Alfa Aesar), calcium oxide powder (99%, Fisher Chemicals), and germanium powder (99.9%, Acros Organics). Distilled calcium was used in several of the reactions; this was prepared by using a custom-built steel vessel with a water-jacketed vacuum attachment, which was attached to a diffusion pump system. Several grams of commercial Ca shot were placed in the steel vessel and heated to 600–620 °C under a dynamic vacuum of 10^{-4} – 10^{-5} Torr to decompose the calcium hydride contaminant and remove the resulting hydrogen gas. The hot

H_2 reacts with any calcium oxide coating on the metal to form water vapor, which is also removed by the vacuum. The calcium was kept under these conditions for about 4 h (until the vacuum level fell below 10^{-5} Torr and maintained the low pressure, indicating the end of hydrogen production), then cooled. The distilled Ca product appeared to be more reflective and metallic than commercial Ca.

Reactants were weighed out and placed into steel crucibles (6.5 mm i.d.), which were arc-welded shut under argon; these ampoules were placed in fused silica jackets sealed under a vacuum of 10^{-2} Torr. A variety of reaction ratios were explored by using both commercial calcium and distilled calcium to make the Ca/Li flux. Small amounts of $\text{LiCa}_7\text{Ge}_3\text{H}_3$ and $\text{LiCa}_{11}\text{Ge}_3\text{OH}_x$ phases were originally found from the reaction of Ge and CaH_2 in a Ca/Li flux formed from commercial calcium contaminated with hydride and oxide; a large amount of the binary phase Ca_2Ge was also produced in this reaction. Addition of larger amounts of CaH_2 as a reactant in this flux (10:10:2:3 mmol ratio of Ca/Li/Ge/ CaH_2) increased the yield of $\text{LiCa}_7\text{Ge}_3\text{H}_3$ and $\text{LiCa}_{11}\text{Ge}_3\text{OH}_x$ (20% based on Ge). The highest yield of $\text{LiCa}_7\text{Ge}_3\text{H}_3$ (50%) was produced by using distilled calcium with deliberate addition of CaH_2 , with a Ca/Li/Ge/ CaH_2 millimolar ratio of 10:10:2:3. The addition of CaO was explored to improve the yield of $\text{LiCa}_{11}\text{Ge}_3\text{OH}_x$. Reactions with a 10:10:2:3:1 millimolar ratio of Ca/Li/Ge/ CaH_2 /CaO produced larger amounts of $\text{LiCa}_{11}\text{Ge}_3\text{OH}_x$; $\text{LiCa}_7\text{Ge}_3\text{H}_3$ was also formed in this reaction.

All reaction ampoules were heated to 1323 K in 2 h and were kept at this temperature for 2 h. They were cooled to 1073 K in 24 h and then cooled to 773 K in 108 h. At 773 K, the tubes were removed from the furnace, inverted, and centrifuged to force the excess molten Ca/Li mixture off of the product crystals. Much of the crystalline product adheres to the surface of the steel crucible during growth and centrifugation, so the use of a filter to separate the crystals from the flux is not necessary. Crucibles were cut open in a glovebox under argon. The solid product consisted of silver-reflective rectangular crystals up to 1 mm long in the case of $\text{LiCa}_{11}\text{Ge}_3\text{OH}_x$ and silver-multifaceted crystals up to 1 mm long in the case of $\text{LiCa}_7\text{Ge}_3\text{H}_3$. These phases were easily visually distinguished from the common byproduct of recrystallized CaH_2 (which grew as clear lath-shaped crystals in increasing yield as the amount of CaH_2 reactant increased). Both phases were extremely air- and water-sensitive. Elemental analysis was performed by using a JEOL scanning-electron microscope with EDS capabilities. This technique cannot analyze light atoms, but the calcium and germanium ratios confirmed those determined from the structure refinements (see below). No iron was detected in the product crystals.

Structure Determination: Powder X-ray diffraction studies were carried out on reaction products to determine identities of byproducts and to explore the effects of changing reaction stoichiometry. Data were collected with an original diffraction setup based on a Huber imaging plate Guinier camera 670 that uses $\text{Cu-K}\alpha_1$ radiation ($\lambda = 1.54060$ Å) with a Ge crystal monochromator. For single-crystal X-ray diffraction studies, small spheroid pieces cleaved from the larger bulk crystals were mounted in cryoloops by using Paratone oil. X-ray diffraction data were collected at 150 K in a stream of nitrogen with a Bruker APEX 2 CCD diffractometer with an $\text{Mo-K}\alpha$ radiation source. Processing of the data was carried out by using the program SAINT; absorption corrections were applied to the data by using the SADABS program.^[18] Refinements of the structures were performed by using the SHELXTL package.^[19] The structure of $\text{LiCa}_7\text{Ge}_3\text{H}_3$ was solved in the orthorhombic space group *Pnma*; details of the refinement can be found in Tables 2 and 3. The cal-

cium and germanium sites were found by direct methods and the lithium and hydrogen sites by analysis of the difference Fourier map and consideration of bond lengths. Anisotropic refinement of thermal parameters was possible for all atoms except for the hydrogen atoms; these were refined isotropically. During the final refinement cycles, occupancies of all atoms were allowed to vary and were not found to vary significantly from unity.

Table 2. Selected crystal data and structural refinement parameters for $\text{LiCa}_7\text{Ge}_3\text{H}_3$ and $\text{LiCa}_{11}\text{Ge}_3\text{OH}_4$.

	$\text{LiCa}_7\text{Ge}_3\text{H}_3$	$\text{LiCa}_{11}\text{Ge}_3\text{OH}_4$
Formula mass [g mol^{-1}]	508.3	695.0
Crystal system	orthorhombic	tetragonal
Space group	$Pnma$	$P4_2/nmc$
Z	4	8
Unit cell parameters [\AA]	$a = 9.8599(2)$ $b = 13.7713(3)$ $c = 8.7430(2)$	$a = 15.832(2)$ $c = 13.694(2)$
Volume [\AA^3]	1187.18(4)	3432.3(8)
Calculated density [g cm^{-3}]	2.844	2.690
Absorption coefficient [mm^{-1}]	10.504	8.552
θ range [$^\circ$]	2.76–34.93	1.82–25.35
Data/restraints/parameters	2682/0/65	1704/0/99
GoF on F^2	1.035	1.052
$R1, wR2$ [$I > 2\sigma(I)$]	0.0195, 0.0405	0.0350, 0.0717
$R1, wR2$ (all data)	0.0248, 0.0421	0.0537, 0.0785
Max., min. residuals [e \AA^{-3}]	0.820, −0.794	0.987, −1.072

Table 3. Atomic coordinates and thermal displacement parameters for $\text{LiCa}_7\text{Ge}_3\text{H}_3$.^[a]

Atom	Wyckoff site	x	y	z	$U_{\text{eq}}^{[b]}$
Ca(1)	8d	0.08986(3)	0.10915(2)	0.05499(3)	0.00771(6)
Ca(2)	8d	0.11268(3)	0.61025(2)	0.32934(3)	0.00724(6)
Ca(3)	8d	0.18597(3)	0.11888(2)	0.45436(3)	0.00661(6)
Ca(4)	4c	0.38456(4)	1/4	0.19600(4)	0.00655(7)
Li(1)	4c	0.1354(4)	1/4	0.7553(5)	0.0147(8)
Ge(1)	8d	0.36828(2)	0.02498(1)	0.21149(2)	0.00740(4)
Ge(2)	4c	0.39418(2)	1/4	0.57552(2)	0.00602(5)
H(1)	4c	0.031(4)	1/4	0.544(4)	[c]
H(2)	4c	0.128(3)	1/4	0.251(3)	[c]
H(3)	4c	0.745(4)	1/4	0.534(4)	[c]

[a] All site occupancies are 100%. [b] U_{eq} is defined as one third of the trace of the orthogonalized U_{ij} tensor. [c] Hydrogen atoms refined isotropically.

Datasets were collected for three crystals of $\text{LiCa}_{11}\text{Ge}_3\text{OH}_x$ from different reactions to determine consistent hydride locations appearing in the difference Fourier maps. For all samples, the structure was solved in the tetragonal space group $P4_2/nmc$ (see Tables 2 and 4). Calcium and germanium sites were found by direct methods. In all three refinements, one Ca site had a lower electron density and was refined as a mixed Ca/Li site, consistently resulting in a 17% Ca/83% Li ratio on this site. The oxygen atom was located as the highest electron-density peak in the difference Fourier map and was assigned as oxygen based on bond lengths and the presence of oxide reactant. Additional refinement cycles and comparison of the resulting difference Fourier maps for the three datasets indicated the consistent presence of three electron-density peaks, which were assigned as hydride sites. During further refinement cycles, no further peaks common to all datasets were seen, although the possibility of additional partially occupied hydride sites cannot be ruled out. Thermal parameters for all atoms were refined anisotropically, except for the hydrogen atoms. Even with isotropic refinement, a negative thermal parameter was observed for two of

the hydride sites. This appeared to have been caused by the extra electron density due to the −1 charge, which made a significant difference for hydrogen. Other reports have approached this problem by fixing the site occupancy factor of hydride sites to 200%.^[14] When this was done in this case, the thermal parameters became positive. The overall stoichiometry of the phase, taking into consideration the Ca/Li mixed site and assuming full occupancy of the hydride sites, is $\text{Li}_{0.826(8)}\text{Ca}_{11.184(8)}\text{Ge}_3\text{OH}_{4.25}$. For ease of discussion and because of the inherent uncertainty in the hydride content, this is approximated as $\text{LiCa}_{11}\text{Ge}_3\text{OH}_x$ ($x \approx 4$) in the manuscript. Further details of the crystal structure investigations can be obtained from the Fachinformationszentrum Karlsruhe, 76344 Eggenstein-Leopoldshafen, Germany [Fax: +49-7247-808-666; E-mail: crysdata@fiz-karlsruhe.de, http://www.fiz-karlsruhe.de/request_for_deposited_data.html] on quoting the depository numbers CSD-422831 (for $\text{LiCa}_7\text{Ge}_3\text{H}_3$) and -422832 (for $\text{LiCa}_{11}\text{Ge}_3\text{OH}_4$).

Table 4. Atomic coordinates and thermal displacement parameters for $\text{LiCa}_{11}\text{Ge}_3\text{OH}_4$.^[a]

Atom	Wyckoff site	x	y	z	$U_{\text{eq}}^{[b]}$
Ca(1)	16h	0.05905(8)	0.11229(8)	0.09624(9)	0.0098(2)
Ca(2)	16h	0.07144(8)	0.02688(8)	0.35106(9)	0.0103(3)
Ca(3)	16h	0.63592(8)	0.06823(3)	0.0014(1)	0.0096(2)
Ca(4)	8g	1/4	0.0223(1)	0.2040(1)	0.0099(4)
Ca(5)	8g	1/4	0.0504(1)	0.7960(1)	0.0212(5)
Ca(6)	8g	1/4	0.1491(1)	0.4104(1)	0.0207(4)
Ca(7)	8g	1/4	0.6422(1)	0.6464(1)	0.0091(4)
Ca(8)	4d	1/4	1/4	0.1564(1)	0.0122(5)
Ca(9)	4c	3/4	1/4	0.5835(1)	0.0096(5)
Li(10)/	8f	0.3507(3)	0.6493(3)	1/4	0.023(2)
Ca(10) ^[a]					
Ge(1)	8g	1/4	0.10010(6)	0.00323(7)	0.0098(2)
Ge(2)	8g	1/4	0.54976(6)	0.42428(7)	0.0101(2)
Ge(3)	8f	0.58886(4)	0.41114(4)	1/4	0.0091(2)
O(1)	8e	0	0	0	0.025(1)
H(1)	2a	1/4	3/4	1/4	[c]
H(2)	16h	0.388(2)	0.518(2)	0.181(2)	[c]
H(3)	16h	0.157(3)	0.136(3)	0.260(4)	[c]

[a] All site occupancies are 100% except for Ca(10)/Li(10) [17.4(8) % Ca, 82.6(8) % Li]. [b] U_{eq} is defined as one third of the trace of the orthogonalized U_{ij} tensor. [c] Hydrogen atoms refined isotropically.

Acknowledgments

This research was supported by the National Science Foundation, under grant award number DMR-05-47791, and by the FSU Department of Chemistry and Biochemistry. This research made use of the scanning electron microscope facility of the FSU Physics Department.

- [1] J. D. Corbett, E. Garcia, A. M. Guloy, W. M. Hurng, Y. U. Kwon, E. A. Leon-Escamilla, *Chem. Mater.* **1998**, *10*, 2824–2836.
- [2] E. A. Leon-Escamilla, J. D. Corbett, *J. Solid State Chem.* **2001**, *159*, 149–162.
- [3] B. Q. Huang, J. D. Corbett, *Inorg. Chem.* **1998**, *37*, 1892–1899.
- [4] a) R. W. Henning, E. A. Leon-Escamilla, J. T. Zhao, J. D. Corbett, *Inorg. Chem.* **1997**, *36*, 1282; b) Q. Liu, R. Hoffmann, J. D. Corbett, *J. Phys. Chem.* **1994**, *98*, 9360–9364.
- [5] E. A. Leon-Escamilla, P. Dervenas, C. Stassis, J. D. Corbett, *J. Solid State Chem.* **2010**, *183*, 114–119.

- [6] E. A. Leon-Escamilla, J. D. Corbett, *Chem. Mater.* **2006**, *18*, 4782–4792.
- [7] E. A. Leon-Escamilla, J. D. Corbett, *Inorg. Chem.* **2001**, *40*, 1226–1233.
- [8] D. T. Peterson, *J. Met.* **1987**, *39*, 20–23.
- [9] M. G. Kanatzidis, R. Pöttgen, W. Jeitschko, *Angew. Chem.* **2005**, *117*, 7156; *Angew. Chem. Int. Ed.* **2005**, *44*, 6996–7023.
- [10] D. A. Lang, J. V. Zaikina, D. D. Lovingood, T. E. Gedris, S. E. Lattner, *J. Am. Chem. Soc.* **2010**, *132*, 17523–17530.
- [11] P. Eckerlin, E. Wölfel, *Z. Anorg. Allg. Chem.* **1955**, *280*, 321–331.
- [12] U. Haussermann, *Z. Kristallogr.* **2008**, *223*, 628–635.
- [13] M. Wendorff, H. Scherer, C. Röhr, *Z. Anorg. Allg. Chem.* **2010**, *636*, 1038–1044.
- [14] M. S. Bailey, M. N. Obrovac, E. Baillet, T. K. Reynolds, D. B. Zax, F. J. DiSalvo, *Inorg. Chem.* **2003**, *42*, 5572–5578.
- [15] M. Knoth, U. Rössler, B. Eisenmann, *Z. Anorg. Allg. Chem.* **2005**, *631*, 1237–1240.
- [16] A. Velden, M. Jansen, *Z. Anorg. Allg. Chem.* **2004**, *630*, 234–238.
- [17] R. D. Shannon, *Acta Crystallogr., Sect. A* **1976**, *32*, 751–767.
- [18] *SAINT*, version 6.02a, Bruker AXS, Inc., Madison, WI, **2000**.
- [19] G. M. Sheldrick, *SHELXTL*, NT/2000, version 6.1, Bruker AXS, Inc., Madison, WI, **2000**.

Received: March 28, 2011

Published Online: July 20, 2011